International Journal of Nanoelectronics and Materials
Volume 14, No. 2, April 2021 [195-208]

Single-phase CZTS thin film prepared by high power impulse magnetron sputtering (HiPIMS): A first attempt

Siti Noryasmin Jaffar[1], Nafarizal Nayan[2*], Zulkifli Azman[2], Amaliyana Raship[2], Mohd Khairul Ahmad[2], Soon Ching Fhong[2], Saidur Rahman[3], Mohd Yazid Ahmad[4], Koichi Sasaki[5]

[1]*Faculty of Electrical and Electronic Engineering, Universiti Tun Hussein Onn Malaysia (UTHM), 86400 Parit Raja, Batu Pahat, Johor, Malaysia*
[2] *Microelectronic and Nanotechnology- Shamsuddin Research Centre (MiNT-SRC), Institute for Integrated Engineering (I²E), Universiti Tun Hussein Onn Malaysia, 86400 Parit Raja, Batu Pahat, Johor, Malaysia*
[3]*Centre for Nano-Materials and Energy Technology (RCNMET), School of Science and Technology, Sunway University, Bandar Sunway, 47500 Petaling Jaya, Malaysia*
[4]*Nanorian Technologies Sdn Bhd, 40 Jln Kajang Perdana 3/2, Taman Kajang Perdana, 43000 Kajang, Selangor*
[5]*Division of Applied Quantum Science and Engineering, Hokkaido University, Kita 13, Nishi 8, Kita-ku, Sapporo 060-8628, Japan*

ABSTRACT

Copper-zinc-tin-sulfide: Cu_2ZnSnS_4 (CZTS) is a non-toxic and abundant materials that could possibly replace the toxic and rare copper-indium-gallium-selenium (CIGS) materials for the absorber of thin film photovoltaic. However, to-date, the CZTS thin film fabrication process is not yet ready for commercialization due to its complexity of quaternary elements. Here, CZTS thin films were deposited for the first time using high power impulse magnetron sputtering (HiPIMS) technique. Although the fabrication of thin film solar cell using conventional DC and RF sputtering is very common, to date, there is no report on the fabrication CZTS thin film using HiPIMS technique. The aim of using HiPIMS system is to resolve the problem on stoichiometry control in single step magnetron deposition, i.e., less composition of zinc and sulphur. The prepared thin films were then characterized using X-ray diffraction (XRD) and atomic force microscopy (AFM). The thickness of each film was measured using a step profiler and verified with a cross-sectional image obtained by FE-SEM. The XRD pattern showed significant different between film prepared by HiPIMS and conventional RF sputtering on single CZTS (112) peaks. The CZTS crystallite size was in the range of 14-28 nm, rely on the discharge power and deposition time. In average, the root mean square roughness was lower than 2 nm, which is useful for solar cell application. The chemical composition analyzed by EDX showed that the atomic ratio of sulfur/metal < 1, indicating that the thin film prepared by HiPIMS deviated from CZTS stoichiometric.

Keywords: single-phase crystallization, CZTS thin film, HiPIMS, magnetron sputtering

1. INTRODUCTION

Cu_2ZnSnS_4 (CZTS) may be a modern compound material that has been offered to supplant harmful components utilized in $CuInGaSe_2$ (CIGS) and CdTe thin film solar cells. A few surveys arise to distribute regarding vacuum and non-vacuum method that have been endeavored for the growth of CZTS thin films [1]–[4]. The proficiency of CZTS-based solar cells, that are manufactured utilizing vacuum or non-vacuum strategies, have been progressed altogether in later decade [5]–

* Corresponding Author: nafa@uthm.edu.my

[7]. Furthermore, research endeavors of industrial producers, such as IBM demonstrates a gigantic approach for marketing the CZTS based solar cells in anytime soon. To date, the most elevated proficiency of 12.6% has been detailed by IBM gather in a solar cell utilizing CZTS as the absorber layer [8]. For commercialization purpose, the solar cell effectiveness of 30% and over is required.

Magnetron sputtering may be a straightforward, dependable strategy to deposit very high quality and large surface thin films with great cardinality. It could be a developed innovation and is broadly utilized in numerous businesses, for example, microelectronics and automobiles [9]–[11]. Subsequently, from the technical perspective, magnetron sputtering could be a favourable method in marketing the generation of CZTS-based solar cells. In any case, the deposition of CZTS thin films utilizing magnetron sputtering has trouble within the stoichiometric issues [12]-[14]. This issue is deemed to be resulted by high vapour pressures of sulphur and zinc. Thus, the deposited CZTS thin film was less composition of sulphur and zinc.

In numerous reviews, the manufacturing of CZTS thin films demand two-step procedure [14-16]. Firstly, a CZTS thin film is deposited employing a vacuum or non-vacuum method. Next, the composition of sulphur is improved by post-annealing treatment in sulphur including environment. Such strategies are complicated and it create harmful effect. In this work, a single-step procedure utilizing high power impulse magnetron sputtering is ideal for synthesizing CZTS thin films. The single-step procedure may also diminish the production expenditure of CZTS-based solar cells and it is best from the industrial perspective. In contrast, to recognize the single-step synthesis of CZTS thin films, it is fundamental to acknowledge its development components in magnetron sputtering deposition. Especially, focusing on the problematic sulphur and zinc contents in CZTS thin film deposition. In addition, our recent finding shows that the sticking probability of sulphur in CZTS sputtering plasma was lower than those of copper, zinc and tin [17]. This may be one of the reasons of less-composition of sulphur in CZTS thin film. Therefore, it is essential to fundamentally acknowledge the growth mechanism of CZTS thin film.

2. HIGH POWER IMPULSE MAGNETRON SPUTTERING (HiPIMS)

Recently, high power impulse magnetron sputtering (HiPIMS) is a new coating innovation with a relatively new principle which includes magnetron sputtering with pulsed power [8]. Huge divisions of sputtered atoms and near-target gases are ionized, by introducing high amplitude power, in pulses, and also a low duty cycle. In comparison to the traditional magnetron sputtering, HiPIMS can be marked by self-sputtering, or rehashed gas recycling for high and low sputter yield materials accordingly. Meanwhile, both characterizations can also be used for most intermediate materials. In front of the target, there is a dense plasma, and this plasma has dual functionality of maintaining the release and giving plasma-assistance to film development, influencing the microstructure of developing films. Most thin films are compound films that are mainly made of oxygen or nitrogen, or can also be composed of other metals and a reactive gas. Minor consequences may emerge for the system when a reactive gas is included; the target may end up being contaminated, i.e., a compound layer that forms on the target surface will influence the sputtering yield and the yield of secondary electron emission, and thus will affect all other parameters. Huge emphasis on the influence on target state; it does not only depend on the partial pressure of the reactive gas used (adjusted through gas flow and pumping), but also on the ion flux to the target, which can be adjusted by the pulse parameters.

For the past several years, high power impulse magnetron sputtering (HiPIMS) evolved into major option for raising functional or good standard of hard films for numbers of applications

[8,10,11]. In order to enhanced the deposition of CZTS thin film with good properties, the advancement of new deposition techniques and comprehensive characterization of CZTS material are essential. Up to now, just several scientific studies had been centered on controlling and tailoring the attributes of CZTS thin films acquired by single target sputtering deposition methods [1-3,9,13,14]. No work has been reported on the usage of HiPIMS for CZTS thin film deposition. HiPIMS is a complex system that requires intensive effort to ignite and control the plasma system.

In the present work, we used a single stoichiometric target of Cu_2ZnSnS_4 sources for thin film deposition using magnetron sputtering plasmas with HiPIMS system. Our HiPIMS system is powered by Starfire Industries (SF-IMPULSE-SH) and backed by PS Plasma DC power supply (SDC 1024A).

3. EXPERIMENTAL SETUP

Cu_2ZnSnS_4 thin films were deposited on silicon wafer p-type (100) substrates using high power impulse magnetron sputtering. The silicon wafer was cut into small pieces of about 1 inch × 1 inch for deposition. Before film deposition, the sputter chamber was evacuated to less than 10^{-3} Pa. A stoichiometric CZTS target with atomic ratio Cu:Zn:Sn:S = 25%:12.5%:12.5%:50% having a diameter of 3 inch and thickness of 1/8 inch was used as sputtering target. The distance between the target and the substrate was about 6 inches, and the substrate holder rotated at fixed frequency of 5 rpm. No additional heat supply to the substrate. Argon gas was applied as working gas during the sputter deposition with a flow of 40 sccm, and the sputtering pressure was kept constant to 1 Pa. The HiPIMS power were varied at 50, 100 and 150 W and the deposition time were varied at 15, 30, 60 and 90 minutes. For the sake of comparison, CZTS film was also deposited using conventional RF magnetron sputtering system for 60 minutes at 100 W. This parameter was chosen to make comparable with HiPIMS result and analysis especially for the deposition rate.

The objective of this particular research consists equally in checking out the outcome on the HiPIMS power discharge and deposition period on structural, electrical and optical qualities and in knowing the correlation appeared among the qualities plus lattice stoichiometry deviation. HiPIMS discharge power impact on morphological, electrical and optical properties. Sputtering power was diverse through a broad selection, over 50 until 150 W, equivalent with the expansion on the deposition ratio over 1 to 10 nm/min. The energy impact on the deposition rate is proved in section 4. It is intended that the speed consecutively rise with increment of sputtering power, therefore greater concentration of the sputtered allergens that comes with extra-energized ions encroaching on the substrate area. The sputtering electrical power perturbation stimulates a stoichiometry deviation within the film composition and it primarily arise to remunerate a far better CZTS thin film. It is speculated that the significant energy improved the dissemination occurrence, and this could encourage an improved CZTS thin film.

The chemical composition, morphology, and crystalline properties of the films were characterized by an energy-dispersive X-ray spectroscopy (EDS), a field-emission-scanning electron microscope (JEOL FESEM J7600) and an X-ray diffractometer (XRD, Panalytical Xpert^2), respectively. The film thickness was evaluated using surface profiler (KLA Tencor, Alpha Step Q) and the surface roughness was evaluated using atomic force microscope (Park System AFM, XE-100). Figure 1 shows the schematic diagram of conventional sputter deposition system attached with HIPIMS system and Table 1 highlights the details experiment of the deposition of CZTS thin film using HIPIMS and RF Magnetron sputtering.

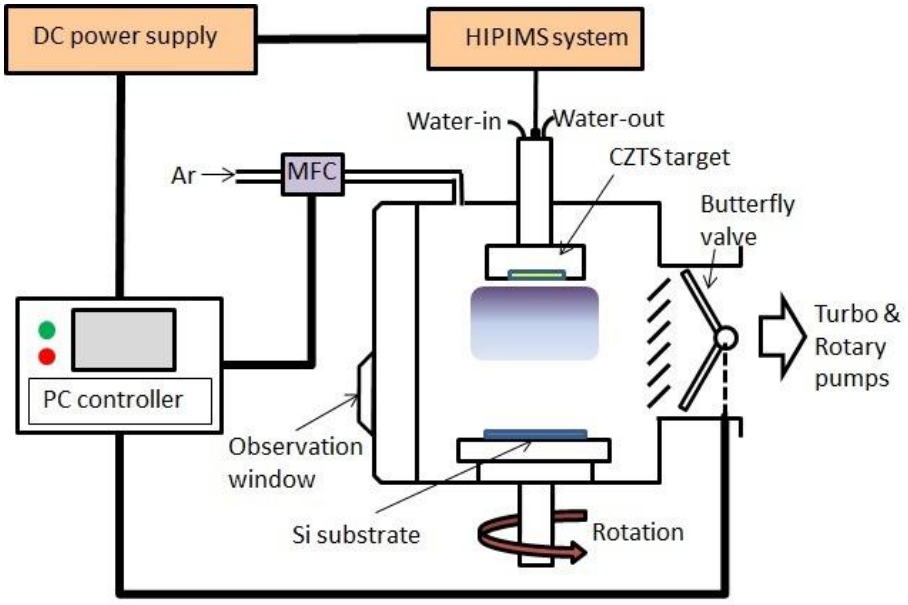

Figure 1. Schematic diagram of conventional sputter deposition system attached with HIPIMS system.

Table 1 The details experiment of the deposition of CZTS thin film using HIPIMS and RF Magnetron sputtering.

Experiment	Effect HIPIMS Power	Effect deposition time	RF Sputtering
Power Source	DC HIPIMS	DC HIPIMS	RF
Average power	50W, 100 W, 150 W	100W	100W
DC Voltage	375 V	380 V	-
Average Current	0.55 A	0.54A	-
Freq.	2000 Hz	2000 Hz	-
Duty Cycle	20us	20us	-
Chamber Base Pressure	4 x 10^{-6} Torr	4 x 10^{-6} Torr	4 x 10^{-6} Torr
Working Pressure	10 mTorr	10 mTorr	10 mTorr
Ar gas flow rate (sccm)	100	100	100
Distance target to substrate	120 mm	120 mm	120 mm
Deposition time	60min	15-90min	60min
Substrate rotation	5 rpm	5rpm	5rpm

4. RESULTS AND DISCUSSION

4.1 Structural Analysis

Figure 2 demonstrate the XRD spectrum of the CZTS thin film deposited on silicon substrate by HiPIMS at various discharge powers. The sharp peak at 2$\boldsymbol{\theta}$=28.442° pointed to the diffraction of (112) plane of kieserite or stannite structure CZTS (PDF no. 26-0575). This peak intensity was found to be far larger than other peaks, exposing a vigorous preferential orientation at (112)

plane. Although, it is really challenging to differentiate the structure within the kieserite and stannite structure due to the XRD patterns of these two structures vary slightly in the splitting of high order peaks, for example (220) and (116) leading from a significantly differ tetragonal distortion (c/2a)[16]. In addition, Figure 2(a) shows the CZTS film deposited using conventional RF magnetron sputtering technique. The RF power was 100 W. No CZTS peak originated from sample was detected in the XRD spectra of film deposited with conventional RF magnetron sputtering. This indicates that the conventionally deposited sample is XRD- or in other words, if there is CZTS crystalline phase, the size of the nanocrystallites is too small or their density is too low to observe.

As shown in Figure 2(a), it is observed that the CZTS (112) peak intensity continuously increases with the increasing HIPIMS power. The higher intensity can be reasoned by better crystallization or higher number of CZTS nanocrystals at higher deposition power which exhibit thicker film of CZTS thin film as reported by previous study(23). The (112) plane of CZTS is thermodynamically more favorable because it offers the least surface energy. Figure 2(b) shows the broadening of XRD spectra for CZTS thin films prepared at various discharge powers. CZTS thin film prepared at low HiPIMS power showed that the film had broader spectrum thus indicating a smaller crystallite size. Table 1 indicates the full width half maximum (FWHM) for (112) plane and its crystallite size evaluated using Scherrer equation:

$$D = \frac{K\lambda}{\beta \cos\theta} \tag{1}$$

where , ***K*** is the Scherrer constant, and **λ** , β and ***θ*** are X-ray wavelength, the Bragg's diffraction angle and the full width at half maxima (FWHM) of the peak corresponding to the " ***θ***" value, respectively. The values of β and ***θ*** of the XRD peaks are estimated by Gaussian fitting (11). As shown in Table 2, by exposure to higher HiPIMS power, the FWHM of CZTS (112) decreases, and the average crystal size gets larger. This was due to the consequence of higher density of the sputtered particles coupled with more energetic ions impinging on the substrate surface with the increasing of sputtering power [18].

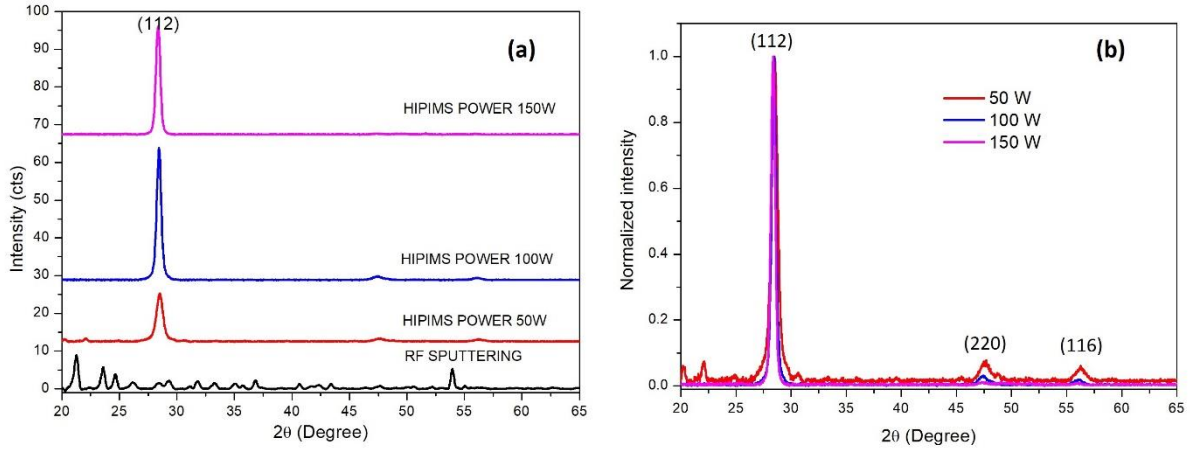

Figure 2. XRD spectra (a) and normalized XRD spectra (b) for CZTS thin film prepared by HiPIMS method at various discharge powers. The deposition time and discharge pressure were fixed at 60 min and 1 Pa, respectively.

Table 2 FWHM and crystallite size of CZTS by the same lattice plane at various powers.

HIPIMS Power (Watt)	Orientation peak	Diffraction angle (°)	FWHM	Crystallite size (nm)
150	(112)	28.442	0.3542	28.28
100	(112)	28.442	0.4864	18.72
50	(112)	28.442	0.6322	15.84
RF SPUTTERING	NA	NA	NA	NA

The deposition time dependence on HiPIMS sputtered CZTS films was also studied. The XRD spectra of CZTS thin films on silicon substrate deposited under various deposition times is shown in Figure 3. The discharge power was fixed at 100 W. The reflection peaks of (1 1 2), (2 2 0) and (1 1 6) planes are formed in all CZTS thin films and the crystalline cubic fluorite structure was obtained for sample deposited more than 15 minutes. Meanwhile there was no CZTS peak formed in the sample deposited at 15 minutes indicating that the film was amorphous film.

Table 3 shows the FWHM and crystallite size of CZTS films prepared at various deposition times. The diffraction peaks become sharper and the intensity increased, indicating the improvement of crystallization of CZTS nanostructure with increasing deposition time. The enhanced peak intensity and narrower FWHM with deposition time are most probably due to the increased excess of CZTS concentration, which results in the formation of larger size of nanostructure. The analysis of the XRD line profile reveals that the thin film consist of nanostructure CZTS, with a typical average crystallite size within 14 nm to 20 nm. Although, there is an exceptional case for sample deposited at 90 minutes, which has the smaller crystallite size compared to sample deposited at 60 min, overall, the crystallite size increases gradually with the deposition time, owing to the increase excess of CZTS concentration.

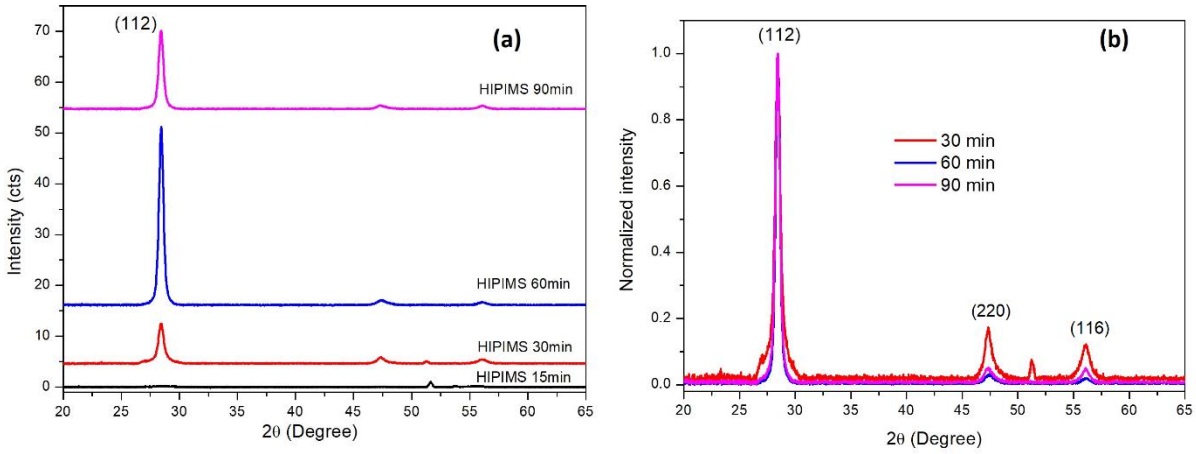

Figure 3. XRD spectra (a) and normalized XRD spectra (b) for CZTS thin film prepared by HiPIMS at various deposition times. The discharge power and pressure were fixed at 100 W and 1 Pa, respectively.

Table 3 FWHM and crystal size of CZTS thin film by same lattice plane at various deposition times.

Deposition time (min)	Orientation peak	Diffraction angle (°)	FWHM	Crystallite size (nm)
90min	(112)	28.442	0.5196	17.53
60min	(112)	28.442	0.4864	18.72
30min	(112)	28.442	0.6471	14.07
15min	NA	NA	NA	NA

4.2 Topological Analysis

The 3D surface visualization of the CZTS thin films deposited on silicon wafer are shown in Figures 4 and 5. In the AFM topography, we can observe the absolute value for the spatial dimension of the CZTS surface. In Figures 4 and 5, the topography and 3D images show granular variations in a very small area ($1 \times 1\ \mu m^2$). Figure 4 shows that the CZTS thin film prepared by HiPIMS and conventional RF sputtering have a smooth surface.

The effect of HiPIMS power on the surface RMS roughness and average grain size are shown in Table 4. The surface roughness of as-deposited CZTS films increases from 1.4 nm to 3.3 nm, while the average grain size increases from 30 nm to 59 nm as the HIPIMS power changes from 50W to 150W. This indicates that the grain size and surface roughness raise with the increment of HIPIMS power. The discharge power controls the energy of incoming atoms during the process of sputtering. Atoms with low energies have poor mobility and create atomic shadowing. Due to the atomic shadowing, atoms are blocked from penetrating the film and filling voids. Hence films with voids are formed and increased the roughness. On the other hand, energetic atoms form dense and compact films by relaxing into voids [19]. The increased surface roughness with sputtering power is related to the larger grain size produced when higher power is used. Meanwhile, there will be more energetic particles strike out the arrived atoms at the surface growing film, which resulting in higher surface roughness with increasing sputtering power [20]. In order to obtain high atomic packaging density and smooth surfaces simultaneously, CZTS films should be deposited at optimized HIPIMS power, which is probably at 100W as shown in Figure 4.

AFM topographical analysis in Figure 5 demonstrates the surface topography of the CZTS deposited at various deposition times. The HIPIMS power was fixed at 100W and the Ar pressure was fixed at 1 Pa. In all cases, nano-grain size are homogeneously distributed all over the substrate surfaces. The surface films deposited at shortest deposition time 15min is rougher than that of films deposited at longer deposition time at 90min. The average surface roughness less than 3 nm has been observed from CZTS films deposited as shown in Table 5. Similar AFM observations were reported by Ghorannevis et al. [20]. The surface roughness decreased with the deposition time.

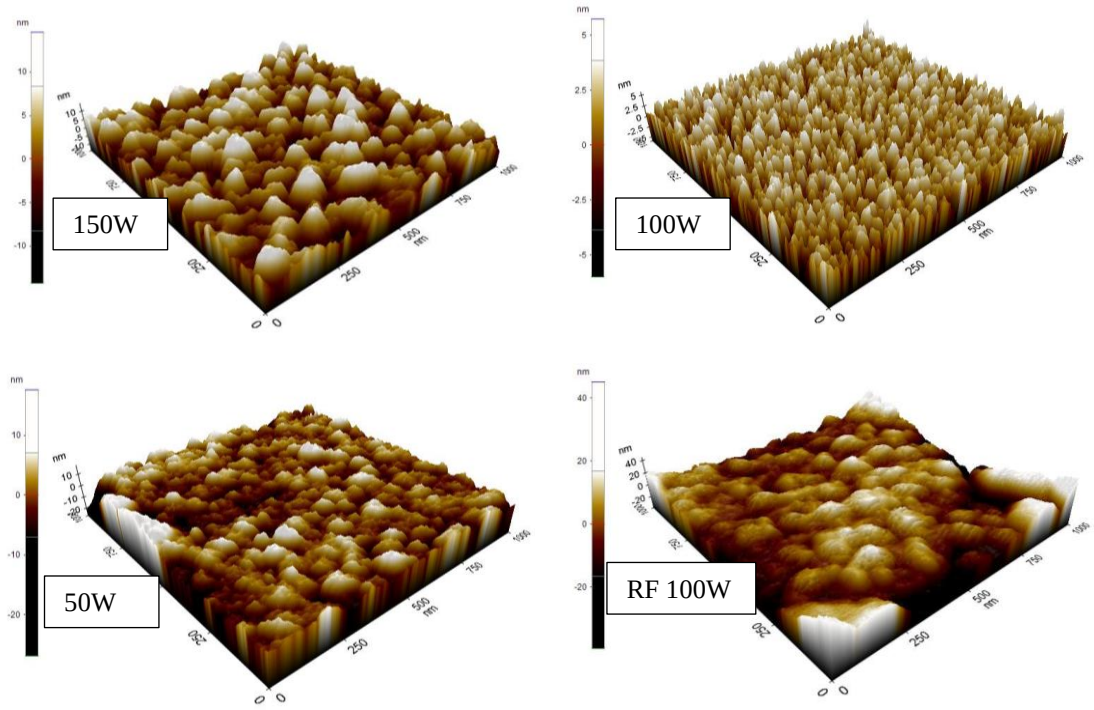

Figure 4. 3D AFM surface visualization of CZTS thin film at various HiPIMS powers. The deposition time and discharge pressure were fixed at 60min and 1Pa, respectively.

Table 4 RMS and grain size of CZTS thin film at various HiPIMS powers.

HiPIMS Power (watt)	RMS (nm)	Grain Size (nm)
150	1.81	58.75
100	1.66	33.72
50	1.43	30.12
RF Sputtering	6.47	32.13

The enhancement in surface smoothness with deposition time from 15min to 90min is attributed to the higher surface atom diffusion. The grain growth and thus the grain size are proportional to the surface diffusion and increases with substrate temperature. Note that it is expected that the substrate holder temperature increased with longer deposition time due to the effect of ions bombardment. As shown in Table 5, it is found that the grain size increases with the deposition time that proved reasonably well to the previous study [21-23]. The increase in the deposition time due to the decrease in the internal micro-strain within the films and an increase in the grain size [22]. The increase in the grain size may be because of the coalescence of small crystals. The grain size was formed by single of million crystallite size. The increment of absorbed atoms mobility resulting the substrate temperature increases which then affect the grain size and crystallinity of the films [23].

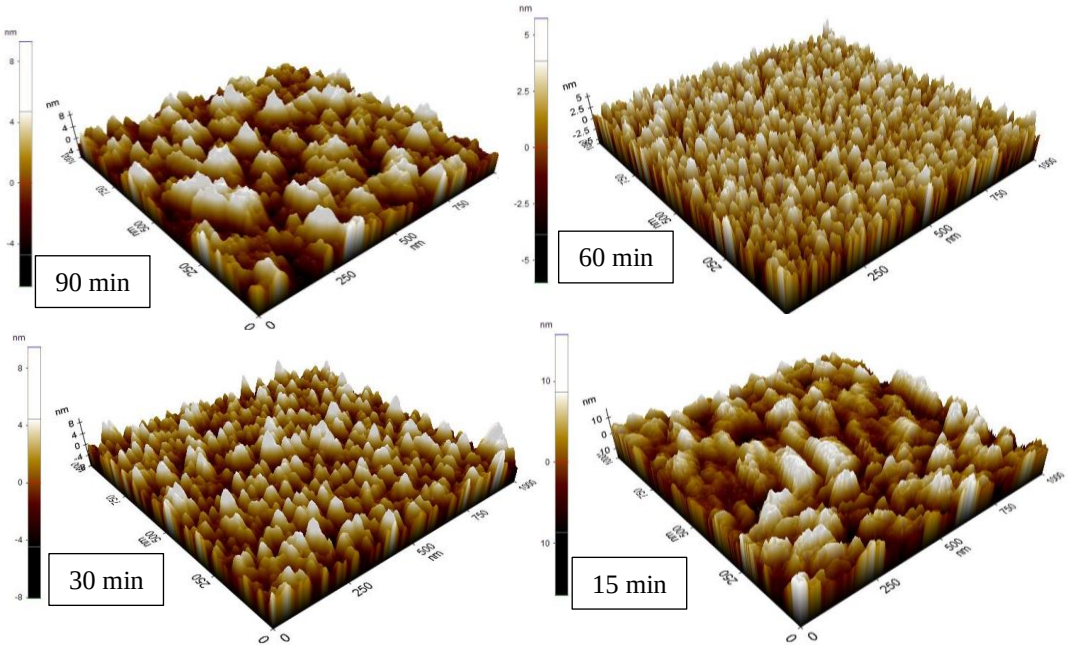

Figure 5. 3D AFM surface visualization of CZTS thin film at various deposition times. The sputtering power and discharge pressure were fixed at 100W and 1Pa, respectively.

Table 5 RMS and grain size of CZTS thin film at various deposition times.

Deposition Time (min)	RMS (nm)	Grain Size (nm)	Thickness (nm)
90	1.45	48.05	78.03
60	1.66	33.72	64.04
30	2.89	13.82	45.13
15	3.11	10.82	20.38

The thickness of CZTS thin film deposited at various deposition times are also shown at Table 5. The CZTS deposition rate obtained for 100 W HiPIMS power was 1.051 nm/min. On the other hand, the deposition rate by conventional RF sputtering was 8.860 nm/min. For the commercialization purpose, it is essential to have a higher deposition rate. Therefore, further study is necessary to improve the deposition rate using HiPIMS system. In addition, Table 5 shows that the grain sizes are related to the film thickness and with increasing thickness; the grain size grows [24].

4.3 Compositional Analysis

The atomic percentages (at. %) of the deposited CZTS film shown in Table 6 is evaluated by EDX analysis resulting the 36.64 atom % Cu, 16.26 atom % Zn, 23.11 atom % Sn, and 25.99 atom % S.

Figure 6 shows EDX element for CZTS thin film prepared by HiPIMS technique. The HiPIMS power and deposition time were 100 W and 60 minutes, respectively. The atomic composition ration of sulfur/metal is far less than 1, indicating that the CZTS film is far from its composition stoichiometric. This film has Cu-rich and S-poor composition as similarly stated for CZTS films by previous research [18]-[20]. It should be observed that despite the stoichiometric target was used for sputtering, the film composition demonstrates some variation from target composition, which may be caused the variance in the sputtering yields of the sputtered species and their sticking probability during the deposition. Note that CZTS films growth by sol–gel [21] and hot injection [22] technique also had S-deficient that is similar to that and was due to the H_2S flow which was not high enough to react with all available metallic Cu–Zn–Sn to Cu_2ZnSnS_4.

Figure 7 shows the field emission scanning electron microscopy (FESEM) micrographs of the surface morphology of the typical CZTS thin film. This film shows a homogeneous, smooth, and extremely dense morphology without any voids and consists of grains with uniform sizes (<100 nm, transverse). Film consists of grains with uniform sizes, although there are several cracks observed due to the aging effect of the film. The surface observation is consistent with the AFM results.

Table 6 Percentage of atomic and weight CZTS thin film. A stoichiometric composition of CZTS is Cu: 25%, Zn:12.5%, Sn:12.5%, S:50%.

ELEMENT	ATOMIC %	WEIGHT %
Copper (Cu)	36.64	30.30
Zinc (Zn)	16.26	13.82
Tin (Sn)	23.11	10.82
Sulfur (S)	25.99	45.05

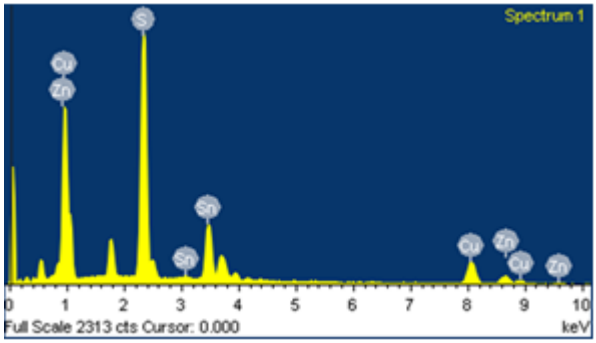

Figure 6. EDX element for CZTS thin film prepared by HiPIMS technique.

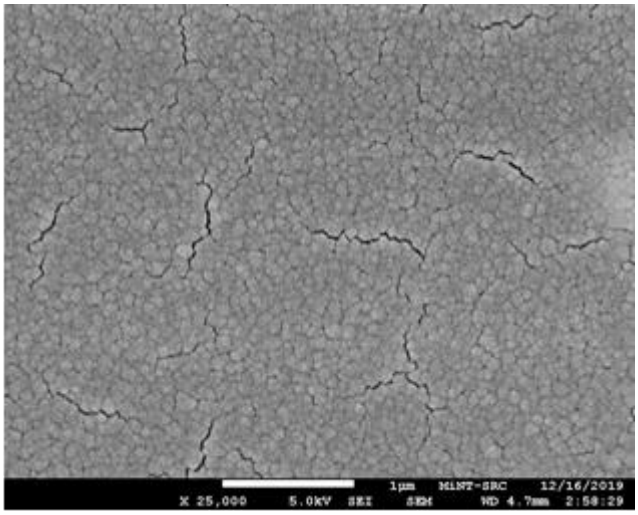

Figure 7. FESEM image of CZTS thin film prepared by HiPIMS technique.

5. CONCLUSION

CZTS thin films were successfully deposited on silicon wafer substrates by HiPIMS sputtering technique and characterized by XRD, AFM, EDX, and FE-SEM. The films exhibit a strong single-phase quaternary CZTS phase preferentially oriented along the (112) plane. These CZTS thin films had a crystallite size of smaller than 30 nm. It also has a smooth, homogeneous and dense surface morphology which is suite for absorber of thin film solar cell. EDX analysis revealed that the thin film prepared was under stoichiometric. Further investigations are necessary to control the stoichiometric composition of CZTS prepared by HiPIMS technique.

ACKNOWLEDGEMENTS

This work was supported by Universiti Tun Hussein Onn Malaysia under GPPS Grant H537 and Ministry of Higher Education Malaysia under PRGS grant K256. Authors also like to express their gratitude towards Mdm Faezahana and Mr Nasrul of Microelectronic and Nanotechnology - Shamsuddin Research Centre for their support on AFM and FE-SEM analysis.

REFERENCES

[1] S. A. Khalate, R. S. Kate, R. J. Deokate, "A review on energy economics and the recent research and development in energy and the Cu2 ZnSnS4 (CZTS) solar cells: A focus towards efficiency" Solar Energy, vol. 169, pp. 616-633, 2018.

[2] M. Ravindiran, C. Praveenkumar, "Status review and the future prospects of CZTS based solar cell – A novel approach on the device structure and material modeling for CZTS based photovoltaic device," Renewable and Sustainable Energy Reviews, vol. 94, pp. 317-329, October 2018.

[3] S. A. Vanalakar, G. L. Agawane, S. W. Shin, M. P. Suryawanshi, K. V. Gurav, K. S. Jeon, P. S. Patil, C. W. Jeong, J. Y. Kim, and J. H. Kim, "A review on pulsed laser deposited CZTS thin films for solar cell applications," J. Alloys Compd., vol. 619, pp. 109–121, Jan. 2015.

[4] Wang, D., Zhao, W., Zhang, Y., Liu, S.F., "Path towards high-efficient kesterite solar cells," Journal of Energy Chemistry, vol. 27, issue 4, pp. 1040-1053, 2018.

[5] H. Fu, "Environmentally friendly and earth-abundant colloidal chalcogenide nanocrystals for photovoltaic applications," Journal of Materials Chemistry C, vol. 6, issue 3, pp. 414-445, 2018.

[6] H. Hiroi, J. Kim, M. Kuwahara, T. K. Todorov, D. Nair, M. Hopstaken, Y. Zhu, O. Gunawan, D. B. Mitzi, and H. Sugimoto, "Over 12% Efficiency CU2ZnSn(SeS)4 Solar Cell Via Hybrid Buffer Layer," 2014 IEEE 40th Photovolt. Spec. Conf., no. I, pp. 30–32, 2014.

[7] Gao S., Jiang Z., Wu L, Ao J., Zeng Y., Sun Y., Zhang Y., "Interfaces of high-efficiency kesterite Cu2ZnSnS(e)4 thin film solar cells," Chinese Physics B, vol. 27 issue 1, pp. 018803, Jan 2018.

[8] Hecimovic, A., Gudmundsson, J.T., "Preface to Special Topic: Reactive high power impulse magnetron sputtering," Journal of Applied Physics, vol. 121, issue 17, pp.171801, 2017.

[9] Shen, T., Chen, Y., Zhu, Y., Gan, G., Yi, J., "Progress in preparation of Cu2 ZnSnS4 thin film by magnetron sputtering," Cailiao Daobao/Materials Review, vol. 30, issue 11, pp. 14-20, 2016.

[10] D. Depla, J. Haemers, and R. De Gryse, "Influencing the hysteresis during reactive magnetron sputtering by gas separation,"Surf. Coatings Technol., vol. 235, pp. 62–67, Nov. 2013.

[11] K. V. Gurav, S. W. Shin, U. M. Patil, M. P. Suryawanshi, S. M. Pawar, M. G. Gang, S. A. Vanalakar, J. H. Yun, and J. H. Kim, "Improvement in the properties of CZTSSe thin films by selenizing single-step electrodeposited CZTS thin films," J. Alloys Compd., vol. 631, pp. 178–182, May 2015.

[12] A. I. Inamdar, S. Lee, K.-Y. Jeon, C. H. Lee, S. M. Pawar, R. S. Kalubarme, C. J. Park, H. Im, W. Jung, and H. Kim, "Optimized fabrication of sputter deposited Cu2ZnSnS4 (CZTS) thin films," Sol. Energy, vol. 91, pp. 196–203, May 2013.

[13] A. Yusupov, K. Adambaev, Z. Z. Turaev, "Some electrical and photoelectric characteristics that are promising for photoconverters p-Cu2ZnSnS4/n-Si heterostructures," Applied Solar Energy (English translation of Geliotekhnika), vol. 51, issue 4, pp. 311-313, Oct. 2015.

[14] Ma, C., Lu, X., Xu, B., Zhao, F., An, X., Li, B., Sun, L., Jiang, J., Chen, Y., Chu, J., "Effects of sputtering parameters on photoelectric properties of AZO film for CZTS solar cell," Journal of Alloys and Compounds, vol. 774, pp. 201-209, 2019.

[15] N. Nafarizal and K. Sasaki, "Sticking probabilities of Cu, Zn, Sn, and S atoms in magnetron sputtering plasmas employing a Cu2ZnSnS4 stoichiometric target," Vacuum, vol. 121, pp. 26-31, 2015.

[16] F. Jiang, H. Shen, W. Wang, and L. Zhang, "Preparation and properties of Cu2ZnSnS4 absorber and Cu2ZnSnS4/amorphous silicon thin-film solar cell," Applied Physics Express, vol. 4, no. 7, Article ID 074101, 2011.

[17] Katagiri, H., Saitoh, K., Washio, T., Shinohara, H., Kurumadani, T. and Miyajima, S., 2001. Development of thin film solar cell based on Cu2ZnSnS4 thin films. Solar Energy Materials and Solar Cells, 65(1-4), pp.141-148.

[18] Tanaka, K., Moritake, N. and Uchiki, H., 2007. Preparation of Cu2ZnSnS4 thin films by sulfurizing sol–gel deposited precursors. Solar Energy Materials and Solar Cells, 91(13), pp.1199-1201.

[19] Vanalakar, S.A., Agawane, G.L., Shin, S.W., Suryawanshi, M.P., Gurav, K.V., Jeon, K.S., Patil,

P.S., Jeong, C.W., Kim, J.Y. and Kim, J.H., 2015. A review on pulsed laser deposited CZTS thin films for solar cell applications. Journal of Alloys and Compounds, 619, pp.109-121.

[20] Moholkar, A.V., Shinde, S.S., Babar, A.R., Sim, K.U., Kwon, Y.B., Rajpure, K.Y., Patil, P.S., Bhosale, C.H. and Kim, J.H., 2011. Development of CZTS thin films solar cells by pulsed laser deposition: influence of pulse repetition rate. Solar Energy, 85(7), pp.1354-1363.

[21] Tanaka, T., Kawasaki, D., Nishio, M., Guo, Q. and Ogawa, H., 2006. Fabrication of Cu2ZnSnS4 thin films by co-evaporation. physica status solidi C, 3(8), pp.2844-2847.

[22] Seol, J.S., Lee, S.Y., Lee, J.C., Nam, H.D. and Kim, K.H., 2003. Electrical and optical properties of Cu2ZnSnS4 thin films prepared by rf magnetron sputtering process. Solar Energy Materials and Solar Cells, 75(1-2), pp.155-162.

[23] Pawar, S.M., Pawar, B.S., Moholkar, A.V., Choi, D.S., Yun, J.H., Moon, J.H., Kolekar, S.S. and Kim, J.H., 2010. Single step electrosynthesis of Cu2ZnSnS4 (CZTS) thin films for solar cell application. Electrochimica Acta, 55(12), pp.4057-4061.

[24] Fernandes, P.A., Salomé, P.M.P. and Da Cunha, A.F., 2009. Growth and Raman scattering characterization of Cu2ZnSnS4 thin films. Thin solid films, 517(7), pp.2519-2523.